

6.5 FECO (Fringes of Equal Chromatic Order)

FECO (Fringes of Equal Chromatic Order)

Ref: Born & Wolf, p. 359.

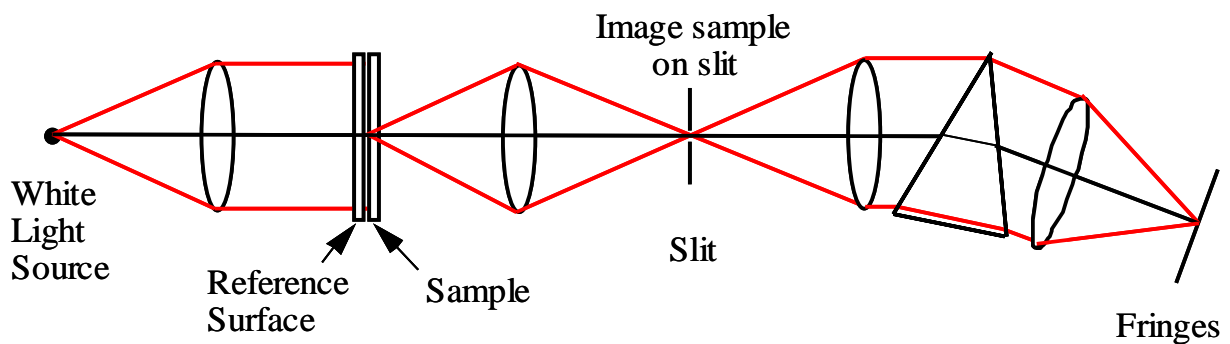
The FECO interferometer is a multiple-beam interferometer in which the test sample is focused onto the entrance slit of a spectrograph. A white light source is used in the interferometer. It can be shown that each fringe gives the profile of the distance between the test surface and the reference surface for the line portion of the surface focused onto the entrance slit.

For multiple-beam interference the transmission is given by

$$I_t = \frac{I_{\max}}{1 + F \sin^2[\delta / 2]} \quad \text{where} \quad \delta = \frac{2\pi}{\lambda_0} 2nd \cos[\theta] + 2\phi$$

ϕ is the phase change on reflection at each surface.

A schematic diagram of a FECO interferometer is shown below. Both the sample and the reference surface must have high reflectivity so high finesse multiple beam interference fringes are obtained. The sample is imaged onto the entrance slit of a spectrograph



If $n = 1$ and $\theta = 0^\circ$ for a bright fringe of order m

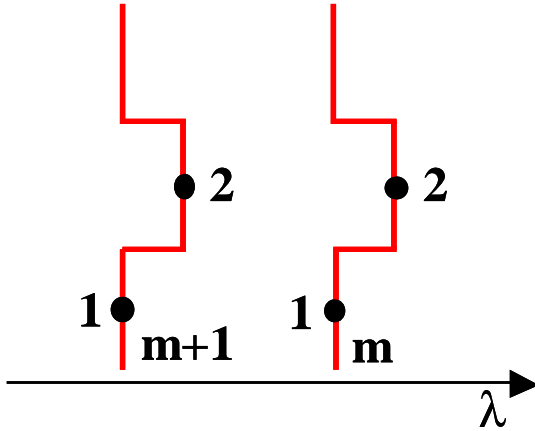
$$\frac{\phi}{\pi} + 2 \frac{d}{\lambda} = m$$

It should be noted that for a given fringe $\frac{d}{\lambda} = \text{constant}$ and

$$\lambda_m = \frac{2d}{m - \frac{\phi}{\pi}}$$

Solving for the height difference across a sample is complicated since $\phi = \phi[\lambda]$. However, with many coatings ϕ can be considered to be independent of λ over the small spectral region used for the analysis. (For more details see Born & Wolf or Jean Bennett, JOSA 54, p. 612 (1964).

The following drawing shows two fringes in the FECO output. The goal is to find the surface height difference between points 1 and 2.



$$d = \left(m - \frac{\phi}{\pi}\right) \frac{\lambda}{2} \quad \text{and} \quad d_2 - d_1 = \left(m - \frac{\phi}{\pi}\right) \left(\frac{\lambda_{2,m} - \lambda_{1,m}}{2}\right)$$

For point 1 and fringe orders m and $m + 1$

$$\left(m - \frac{\phi}{\pi}\right) \lambda_{1,m} = \left(m + 1 - \frac{\phi}{\pi}\right) \lambda_{1,m+1}$$

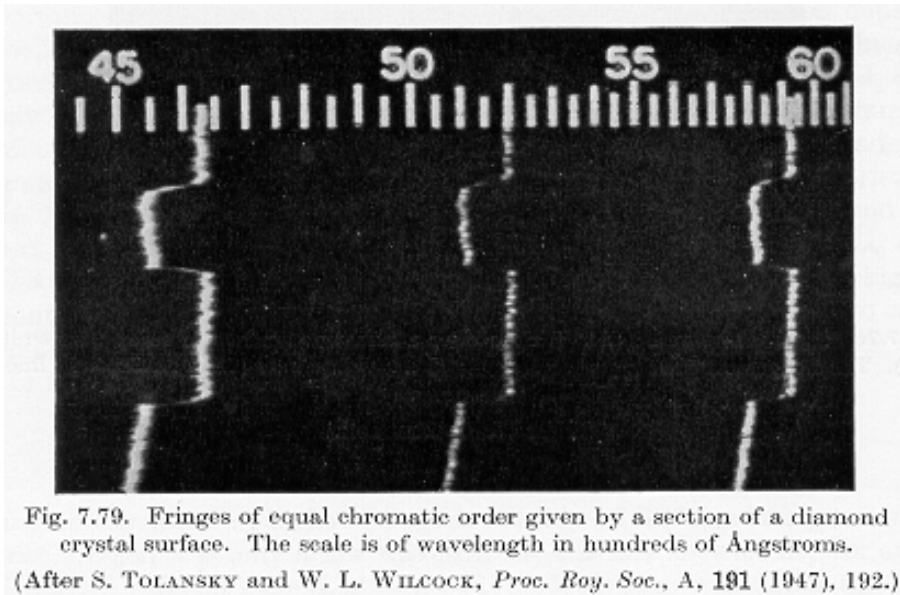
Thus,

$$\left(m - \frac{\phi}{\pi}\right) = \frac{\lambda_{1,m+1}}{\lambda_{1,m} - \lambda_{1,m+1}}$$

and

$$d_2 - d_1 = \frac{\lambda_{1,m+1}}{\lambda_{1,m} - \lambda_{1,m+1}} \left(\frac{\lambda_{2,m} - \lambda_{1,m}}{2}\right)$$

The following figure shows some actual FECO interference fringes (Ref: Born & Wolf).



Since $d_2 - d_1$ is proportional to $\lambda_{2,m} - \lambda_{1,m}$, the profile of the cross-section of an unknown surface is obtained by plotting a single fringe on a scale proportional to the wavelength.

The spectroscopic slit is in effect selecting a narrow section of the interference system and each fringe is a profile of the variation of d in that section since there is exact point-to-point correspondence between the selected region and its image on the slit.

Small changes in d are determined by measuring small changes in λ . There are no ambiguities as to whether a region is a hill or a valley. There are no ambiguities at a discontinuity as we would have with monochromatic light where it is difficult to determine which order belongs to each fringe. Surface height variations in the Angstrom range can be determined.

Two disadvantages are

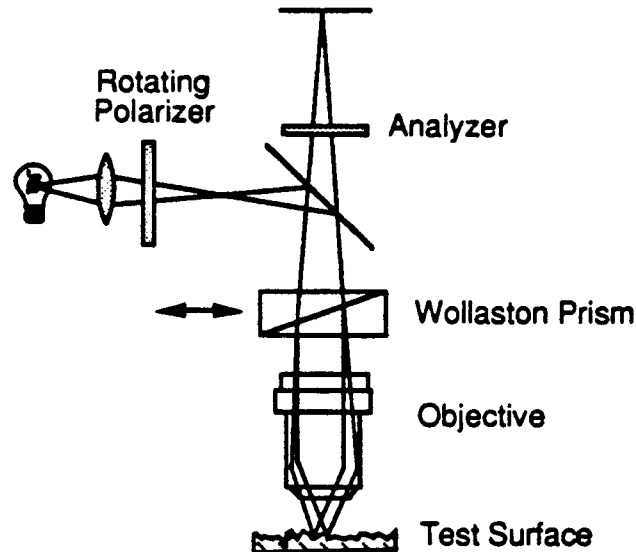
- 1) we are getting data only along a line and
- 2) the sample being measured must have a high reflectivity.

6.6 Nomarski Interferometer

Ref: Francon & Mallick, Polarization Interferometers, p. 69

Nomarski Microscope

The diagram below shows a drawing of the optical layout of a Nomarski microscope. The Nomarski microscope is sometimes called a differential interference contrast (DIC) microscope or a polarization interference contrast microscope.

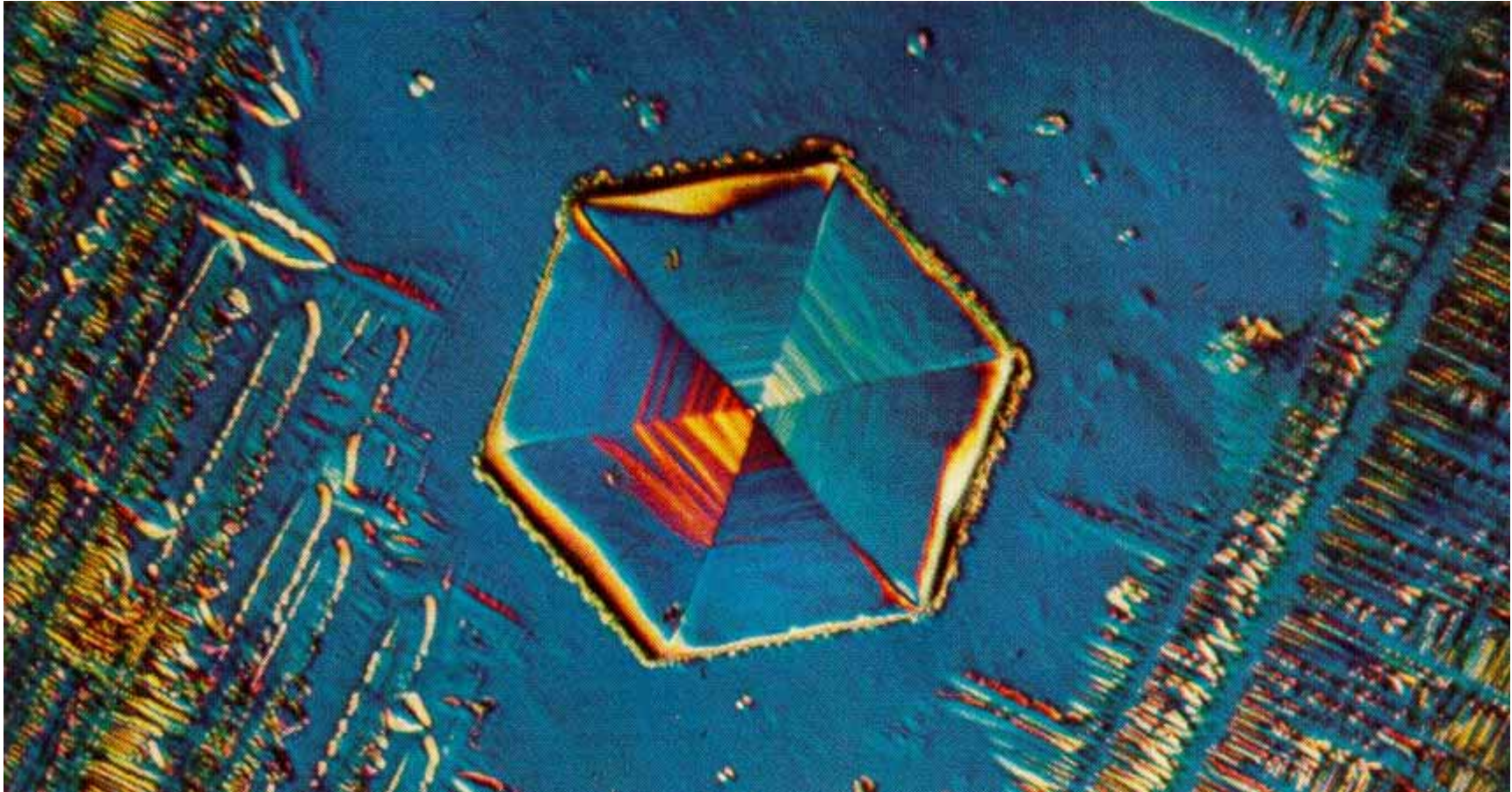


A polarizer after a white light source is used to set the angle of the polarized light incident upon a Wollaston prism. The Wollaston splits the light into two beams having orthogonal polarization, which are sheared with respect to one another. After reflection off the test surface the Wollaston recombines the two beams. A fixed analyzer placed after the Wollaston transmits like components of the two polarizations and generates an interference pattern.

The resulting image shows the difference between two closely spaced points on the test surface. The point separation (shear at the test surface) is usually comparable to the optical resolution of the microscope objective and hence only one image is seen. The image shows slope changes and it appears as though the surface has been illuminated from one side. Like a shearing interferometer, only detail in the direction perpendicular to the shear is seen. In other words, if the shear is in the x direction, only features parallel to the y-axis will be seen. Detail parallel to the x direction will not be visible without rotating the test surface or the Wollaston prism.

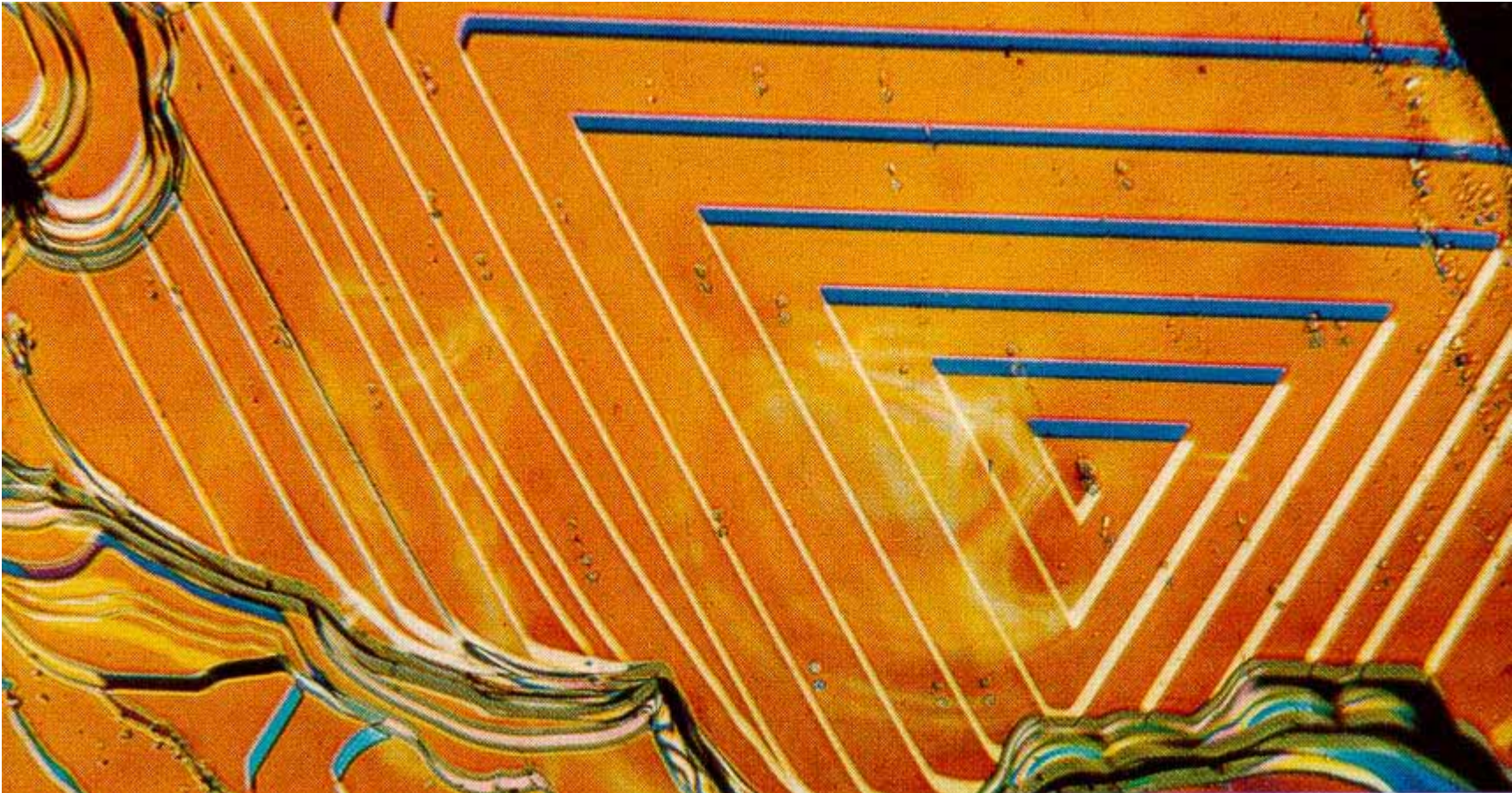
The path difference between the two beams can be adjusted by laterally translating the Wollaston prism. When the axes of the polarizer and analyzer are parallel and the prism is centered, the path lengths are equal and white light is seen for a perfect test surface with no tilt. When the polarizer and analyzer are crossed and the prism centered, no light gets through. When the prism is translated sideways, the two beams have unequal paths and different colors are seen. The color for a specific feature on the test surface depends upon the path difference between the two beams for that point. The color changes indicate the surface slopes. When the polarizer before the prism is rotated, the relative intensities of the two orthogonal polarized beams change, and the colors change.

Crystals of ammonium alum seen with differential polarization microscope



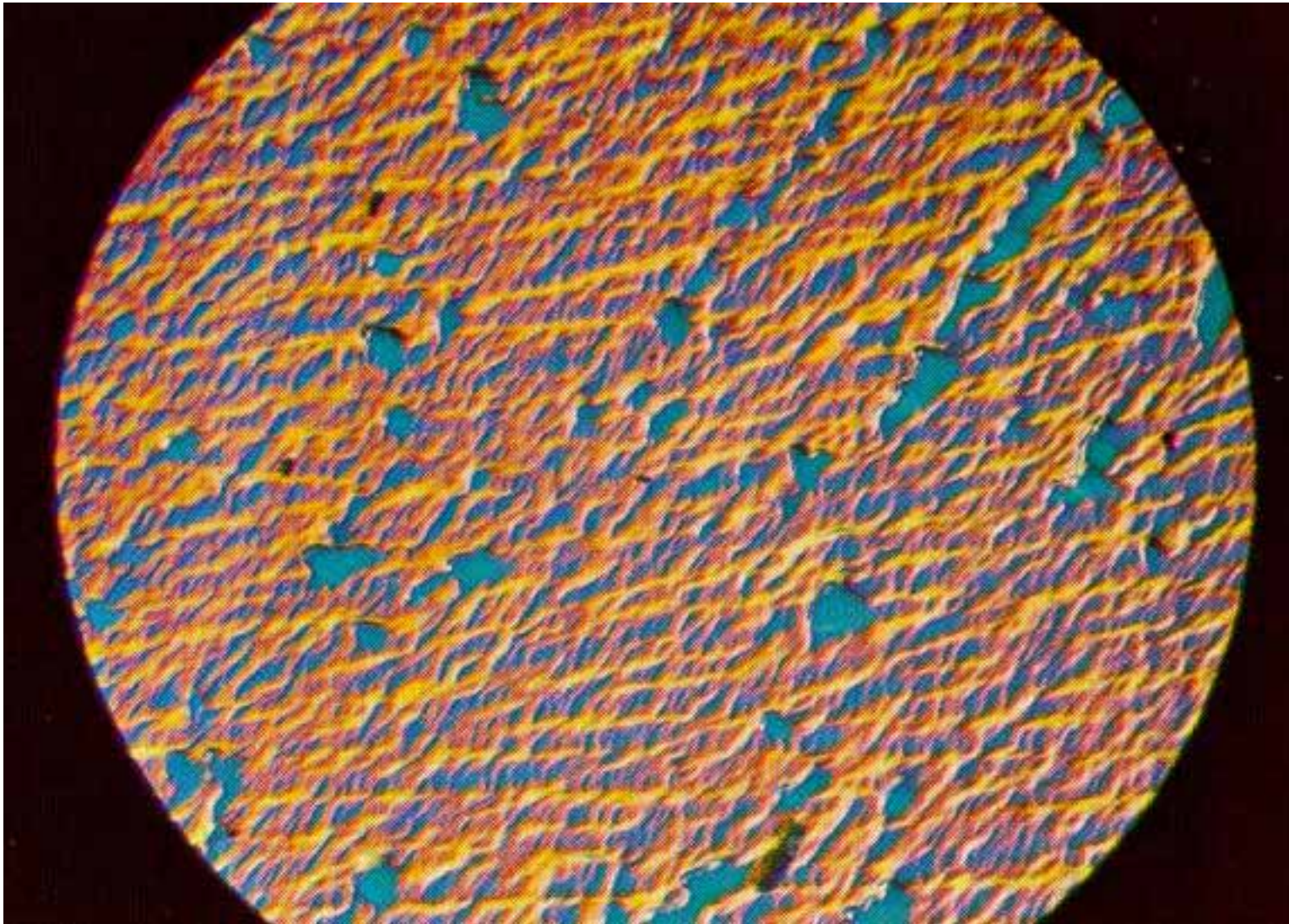
Ref: "Atlas of Optical Phenomena", Vol. 2, Francon et al.

Crystals of silicon carbide seen with differential polarization microscope

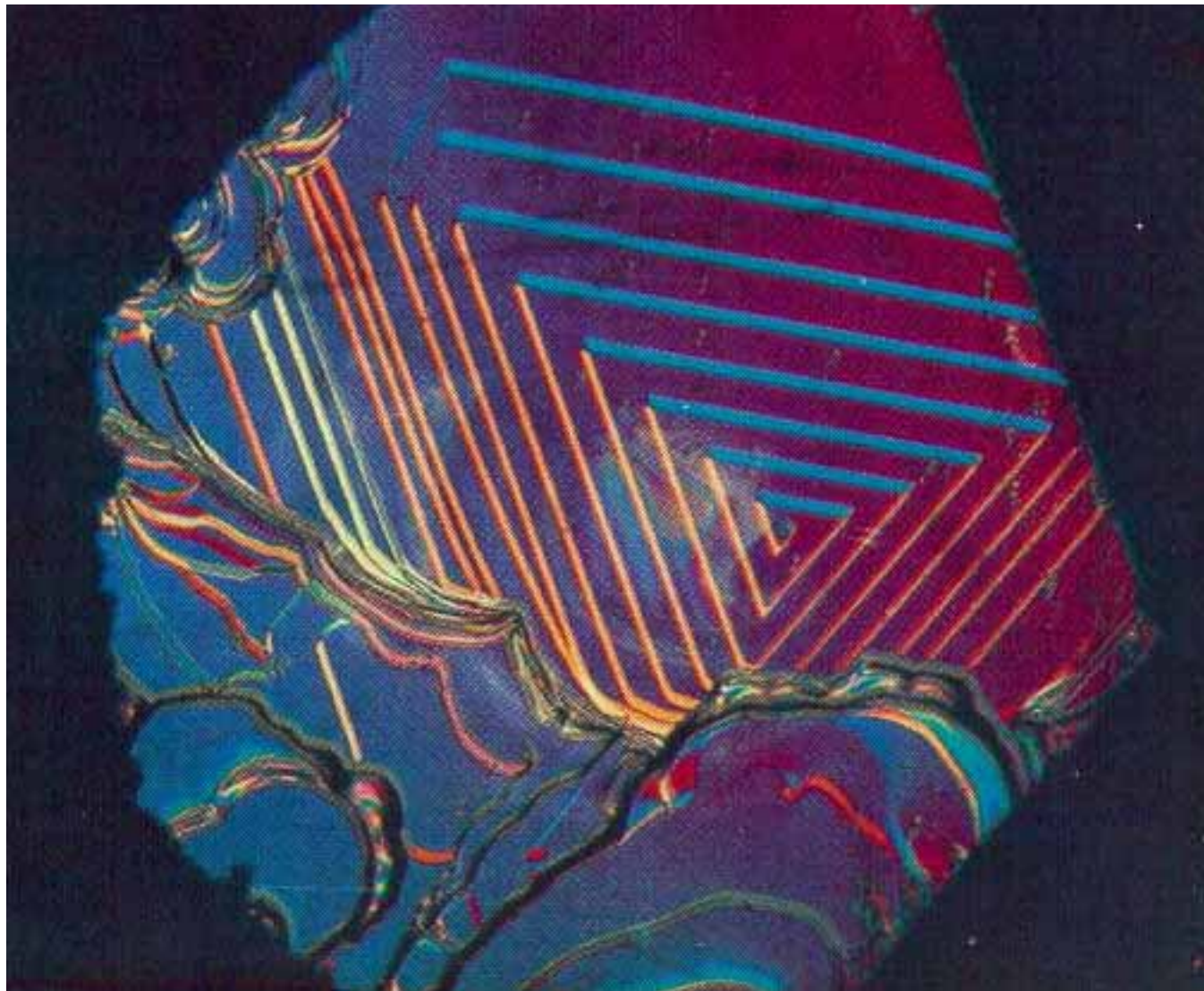


Ref: "Atlas of Optical Phenomena", Vol. 2, Francon et al.

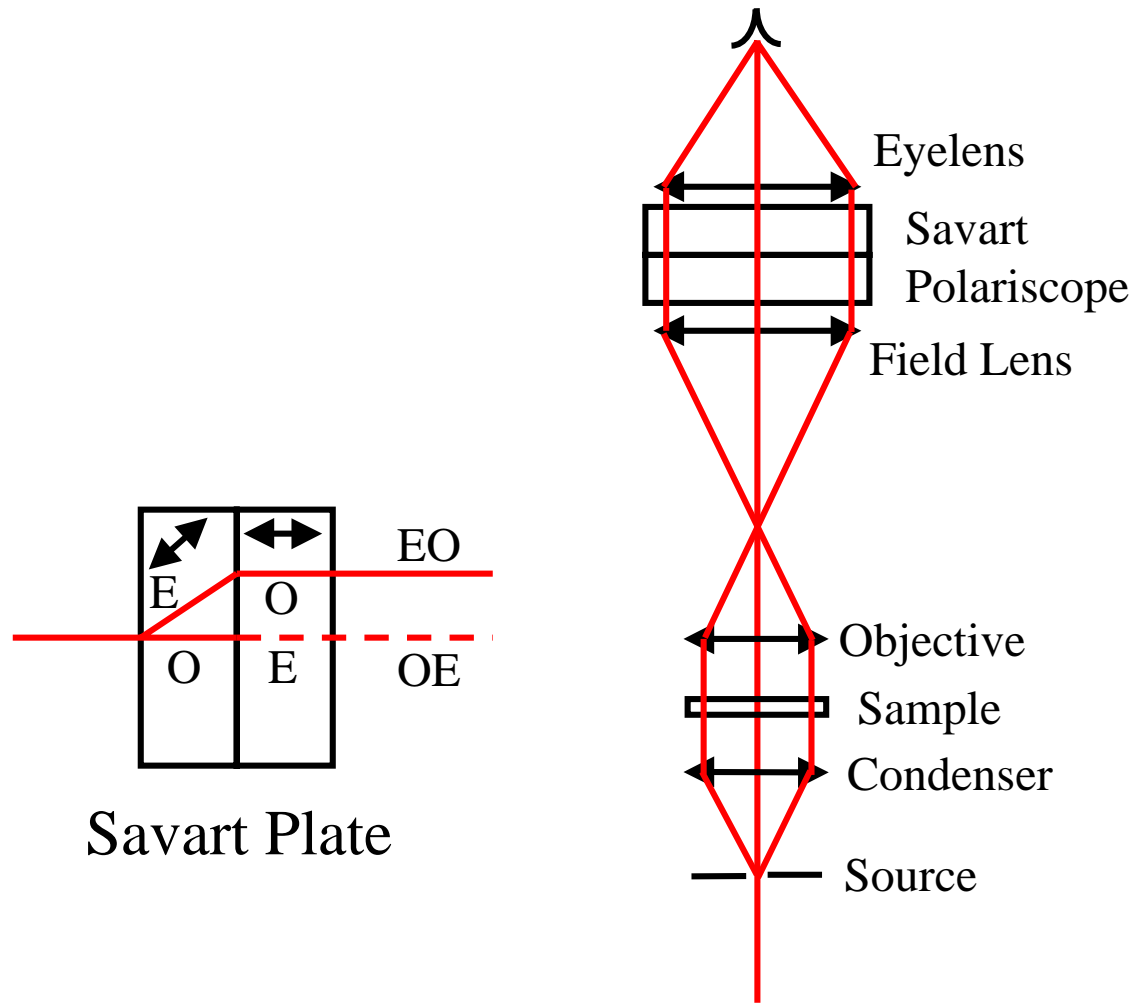
Defects of germanium plate seen with differential polarization microscope



Silicon carbide crystal seen with differential polarization microscope



Francon Interference Eyepiece



6.7 Sommargren

Ref: Applied Optics, 15 February 1981, p. 610

Optical heterodyne profilometry

Gary E. Sommargren

A noncontact optical technique for the measurement of surface profile is described, which has a height sensitivity of the order of 1 Å. It is based on a common path heterodyne interferometer in which two orthogonally polarized beams of slightly different frequency are focused on the surface to be measured. One focal point acts as a reference as the other point circularly scans the surface. The phase of the beat frequency of the interfering return beams is directly proportional to the surface height. The results of a surface measurement include graphical displays of the surface profile, autocovariance function, spectral density function, stability, and repeatability. Comparison with other instruments is also discussed.

I. Introduction

The ability to measure surface roughness is very important in optical polishing when low-scatter high-laser damage-resistant surfaces are desired. Many quantitative methods have been developed and are reviewed in an excellent paper by Bennett.⁷ Of these FECO interferometry,^{1,2} angular dependent scatter,³⁻⁵ total integrated⁶⁻⁸ scatter, and stylus instruments^{9,10} have received the greatest attention. By their nature, the scatter methods give statistical information about the surface and only after assumptions have been made about the height distribution of the surface profile. The FECO method requires the surface to be coated with a highly reflecting film and compared with a reference surface, the quality of which limits the sensitivity of the measurement. The stylus method, perhaps the most sensitive, requires surface contact involving extremely high local pressures. Surface deformation affects the measurement and usually results in a scratch.

This paper describes a noncontact method of measuring surface profile, without need for a reference surface, that is capable of height sensitivities of the order of 1 Å. It does not require any surface preparation and can be used with highly reflecting surfaces as well as bare glass surfaces. Because the surface profile is measured directly, the autocovariance function, spectral density function, and statistical properties of the surface can be determined analytically. The following sections will describe the principles of this method and their incorporation into an instrument, data acquisition and analysis, graphical outputs, sources of errors, limits on sensitivity, repeatability, and comparison with other instruments.

II. Principle of Operation

The basic principle involved in this surface profile measuring method is heterodyne interferometry. When a surface is illuminated by two focused beams of light of slightly different frequency and the reflected beams interfere, the phase of the sinusoidal intensity modulation is related to the height difference between the illuminated points on the surface. If one of the beams remains focused on a fixed point while the other beam is moved along the surface, height variations along the scanned line are measured. The following subsections describe the details of this method.

A. Optical System

The optical system used to implement the principle outlined above is shown in Fig. 1. The light source, shown in Fig. 2, is a single-mode He-Ne laser with its center frequency Zeeman split by an axial magnetic field on the laser tube. The laser is stabilized in two respects: a phase lock loop is used to control the strength of the magnetic field so as to lock the Zeeman frequency to a reference crystal; the relative intensities of the two frequencies are used to control the length of the laser cavity so as to keep them centered on the gain curve, thus stabilizing their absolute frequencies. The laser output consists of two collinear orthogonally linearly polarized beams with a frequency difference of 2 MHz. These beams pass through a telescope/spatial filter to remove spatial noise and reduce their diameter. A polarization insensitive beam splitter¹¹ reflects a small fraction of each beam through a pair of wave plates that serve as an adjustable phase bias and a polarizer oriented at 45° to each polarization, permitting them to interfere at the reference photodetector.

The transmitted beams are directed vertically by a pair of adjustable mirrors to an interferometer comprised of a Wollaston prism, microscope objective, and the surface being measured. The Wollaston prism introduces an angular divergence between the orthogo-

The author is with University of California, Lawrence Livermore National Laboratory, P.O. Box 808, Livermore, California 94550.

Received 30 June 1980.

0003-6935/81/040610-09\$00.50/0.

© 1981 Optical Society of America.

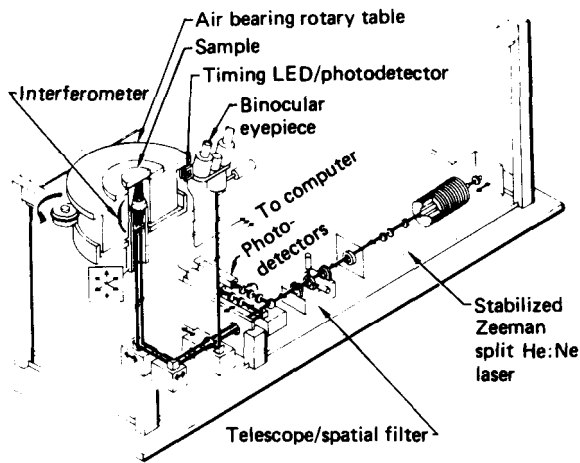


Fig. 1. Schematic of optical system.

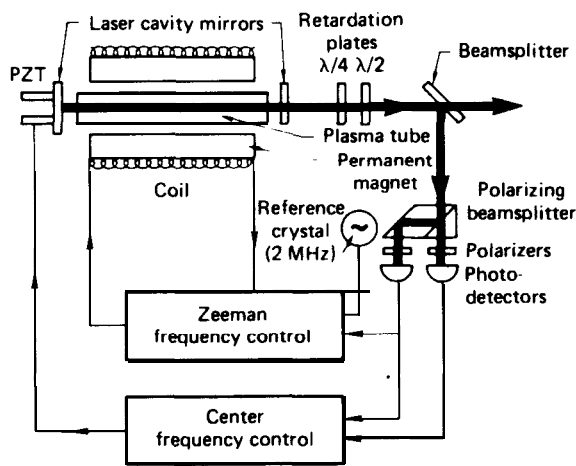


Fig. 2. Zeeman split He-Ne laser and stabilization controls.

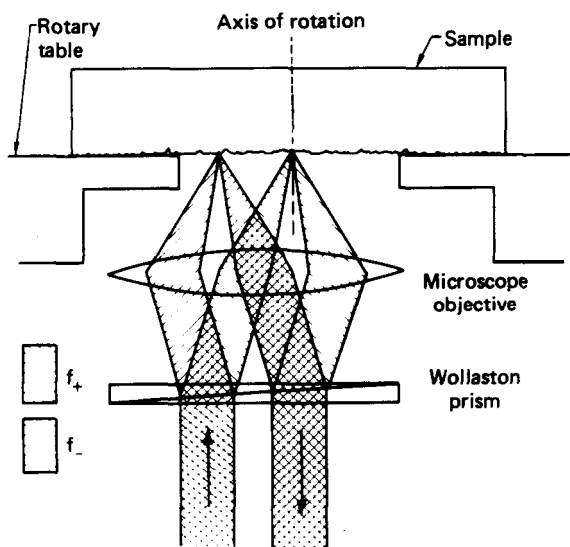


Fig. 3. Detail of interferometer.

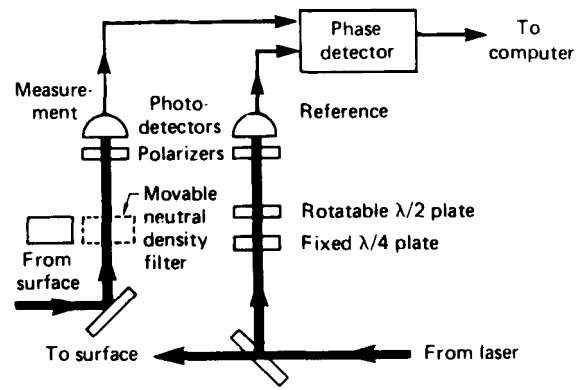


Fig. 4. Detail of phase detection.

nally polarized beams so that the objective brings them to focus at two distinct points on the surface, one on either side of the optic axis with one on the axis of rotation of the rotary table as shown in Fig. 3. The points are separated by $\sim 100 \mu\text{m}$, and the lateral resolution of each beam is $\sim 2 \mu\text{m}$. The reflected beams are recombined by the Wollaston prism and leave on a path parallel to the incident beams but displaced to eliminate overlap. This physical separation is required to prevent light from returning directly to the laser and causing cavity detuning. The beams pass through an adjustable neutral density filter to compensate for surface reflectivity and a polarizer to the measurement photodetector as shown in Fig. 4.

B. Phase/Height Detection

The amplitude of the field at either photodetector can be expressed by

$$V = V_+ + V_- = \exp[i(k_+z_+ - \omega_+t)] + \exp[i(k_-z_- - \omega_-t)], \quad (1)$$

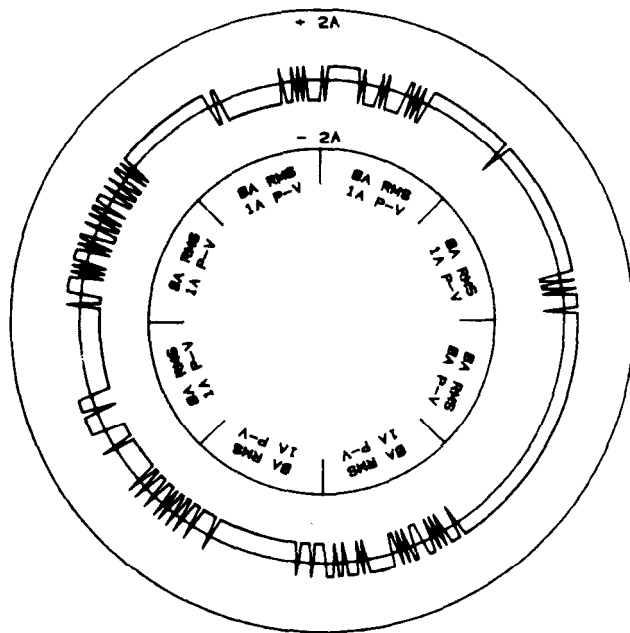
where ω is the angular frequency, k is the wave number, z is the distance traveled, and subscripts $+$ and $-$ correspond to the up-shifted and down-shifted beams. The signal S from each photodetector is proportional to the irradiance $I = |V|^2$. The signal from the reference photodetector is given by

$$S_r = |\exp[i(k_+z_r - \omega_+t - 2\theta)] + \exp[i(k_-z_r - \omega_-t + 2\theta)]|^2 \\ = 2[1 + \cos[(k_+ - k_-)z_r - \omega't - 4\theta]], \quad (2)$$

where $z_+ = z_- = z_r$ is the common path length traveled by the reference beams, $\omega' = \omega_+ - \omega_-$ is the angular Zeeman frequency, and θ is the angular position of the halfwave plate (see Appendix A). The signal from the measurement photodetector is given by

$$S_m = |\exp[i(k_+(z_m + z/2) - \omega_+t)] \\ + \exp[i(k_-(z_m - z/2) - \omega_-t)]|^2 \\ = 2\left[1 + \cos[(k_+ - k_-)z_m + \frac{(k_+ + k_-)}{2}z - \omega't]\right], \quad (3)$$

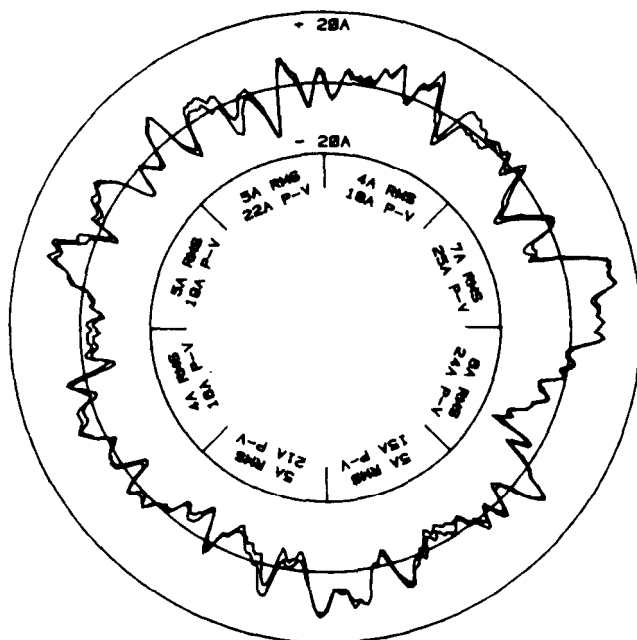
where $z_+ = z_m + z/2$ and $z_- = z_m - z/2$ are the path lengths traveled by the measurement beams, with z_m being the average path length and z being the difference in path lengths. The phase difference ϕ between these signals is



Surface profile

5. 5A RMS 1A P-V 5A ASTIG

Fig. 9. Stability test of system.



Surface profile

5. 5A RMS 38A P-V 4A ASTIG
5. 3A RMS 28A P-V 4A ASTIG

Fig. 10. Repeatability test of system.

ometer, made specifically for this purpose, the average height measured by several observers was 915 Å. The difference between these measurements is less than the stated accuracy of the interferometer.

The accuracy for relatively small surface variations of several angstroms is more difficult to determine because comparison instruments are not commonplace and generally do not lend themselves to automated data analysis. A computer interfaced stylus instrument at the Naval Weapons Center was used to measure two bare glass surfaces. Data were taken on a single linear scan and averaged to simulate a 2- μ m diam spot size. A comparison of the rms surface height, rms slope, and first zero crossing of the autocovariance function is shown in Table II. Although this comparison is by no means exhaustive, the rms surface heights agree within the noise levels of the instruments. The rms slopes and autocovariance lengths, which are more sensitive to the lateral resolution of the measuring instrument, show larger discrepancies. A more intensive study would be needed to determine the source of these differences.

IV. Comments

Every technique used to measure surface profile, whether based on mechanical contact, visible light, x rays, electron beams, capacitance, or magnetic fields, averages over some finite lateral area. In the technique described in this paper, diffraction limits the resolution to $\sim 2\text{-}\mu\text{m}$ spot so that the measured height at a particular surface point is actually a weighted average over the spot size. Thus, the lateral extent of the averaged area is $\sim 20,000$ times the height sensitivity. At first this may appear to be a meaningless measurement; however, it must be realized that lateral surface structure has little or no effect on the performance of the surface when it is less than the wavelength of the light used with the surface, whereas vertical surface variations of the order of angstroms will have a measurable effect. Therefore, for surfaces used in the visible and IR parts of the spectrum, the pertinent information lost by averaging over a 2- μm diam area is minimal.

I wish to thank Cecil Howard for the mechanical design and assembly of the instrument, J. Bob Brown for the overall electronic design and layout, and Bruce Nappi and Richard Young for laser and photodetector additions and modifications. I am grateful to Jean Bennett of Michelson Laboratory, Naval Weapons Center, China Lake, Calif. for measuring samples on a stylus instrument that she has modified and interfaced to a computer.

Parts of this paper were presented at the 1979 Annual Meeting of the Optical Society of America in Rochester, N.Y. [J. Opt. Soc. Am. 69,1404A (1979)].

This work was performed under the auspices of the U.S. Department of Energy by the Lawrence Livermore National Laboratory.

Appendix A: Optically Variable Phase Bias

Phase detectors typically have a range of 2π rad over which there are no ambiguities. When making measurements it is desirable to have the average phase value

6.8 Interference Microscope

Any interferometer can be incorporated in a microscope to give an interference microscope.

Examples

- Mirau
- Michelson
- Linnik
- Multiple Beam

Non-Contact Optical Profilers for Measurement of Surface Microstructure

• Advantages

Non-contact measurement
2D or 3D surface topography
Visual qualitative surface inspection
Vertical resolution suitable for super-polished optics
Fast measurement and analysis

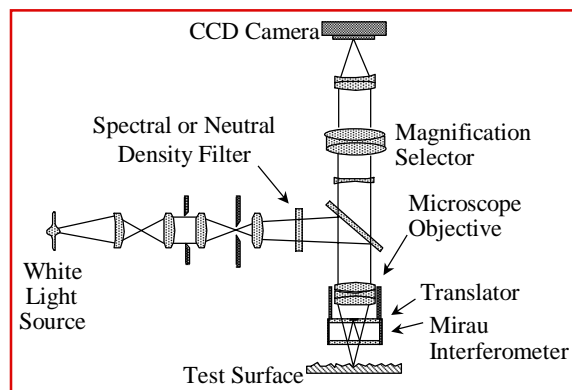
• Disadvantages

Measures phase change as well as profile
Lateral resolution limited by optical resolution

Advantages of White Light over Laser Light

- Lower noise**
No spurious fringes
- Multiple wavelength operation**
Measure large steps
- Focus easy to determine**

Profiler Optical Diagram



Optics 513 - James C. Wyant

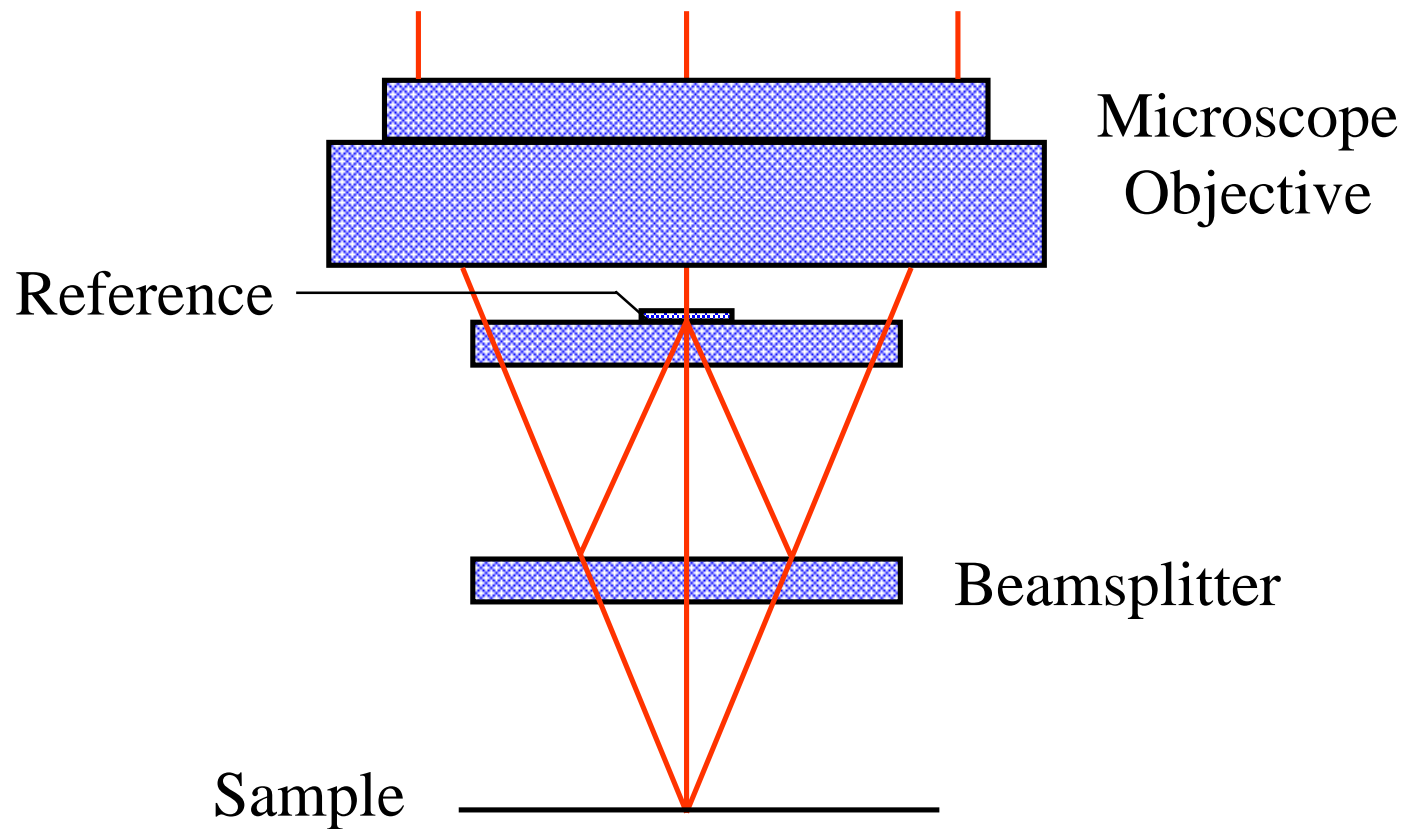
Optical Profiler



Optics 513 - James C. Wyant

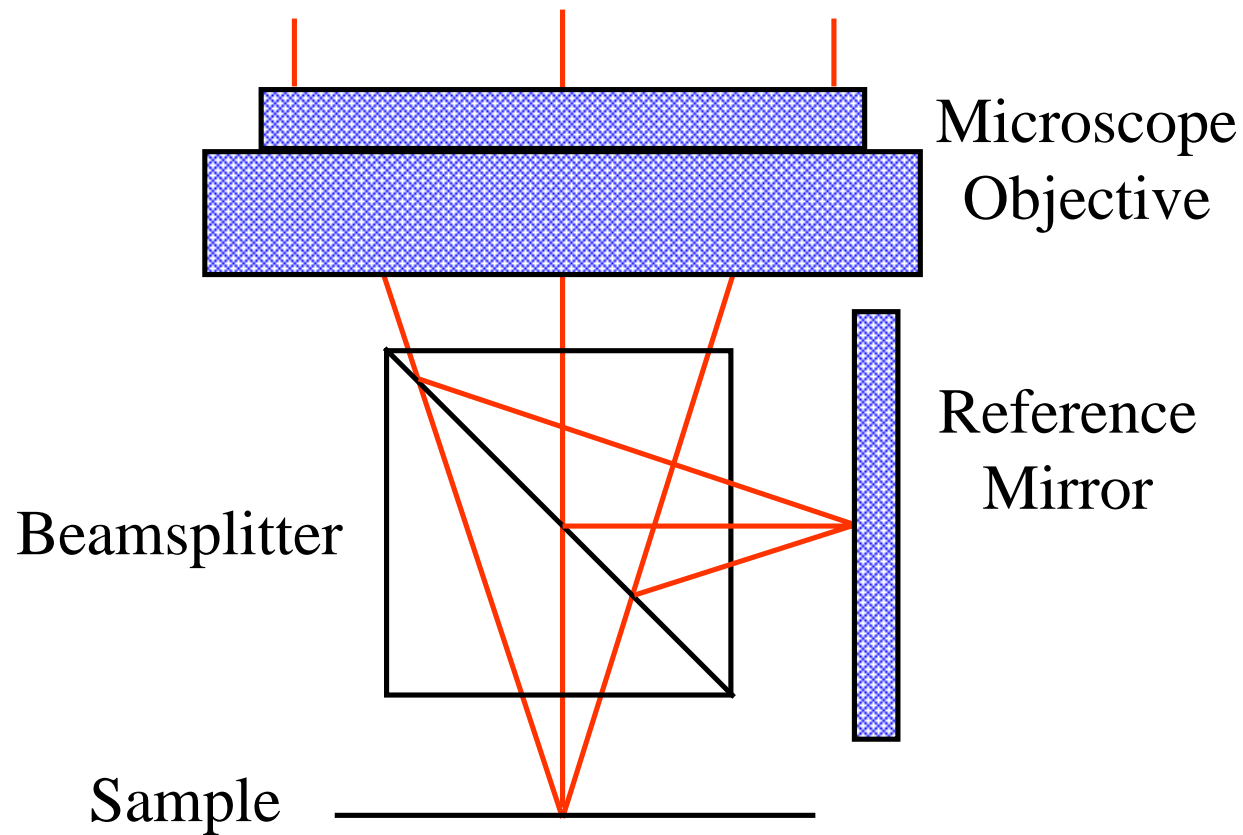
Mirau Interferometer

(10X, 20X, 50X)



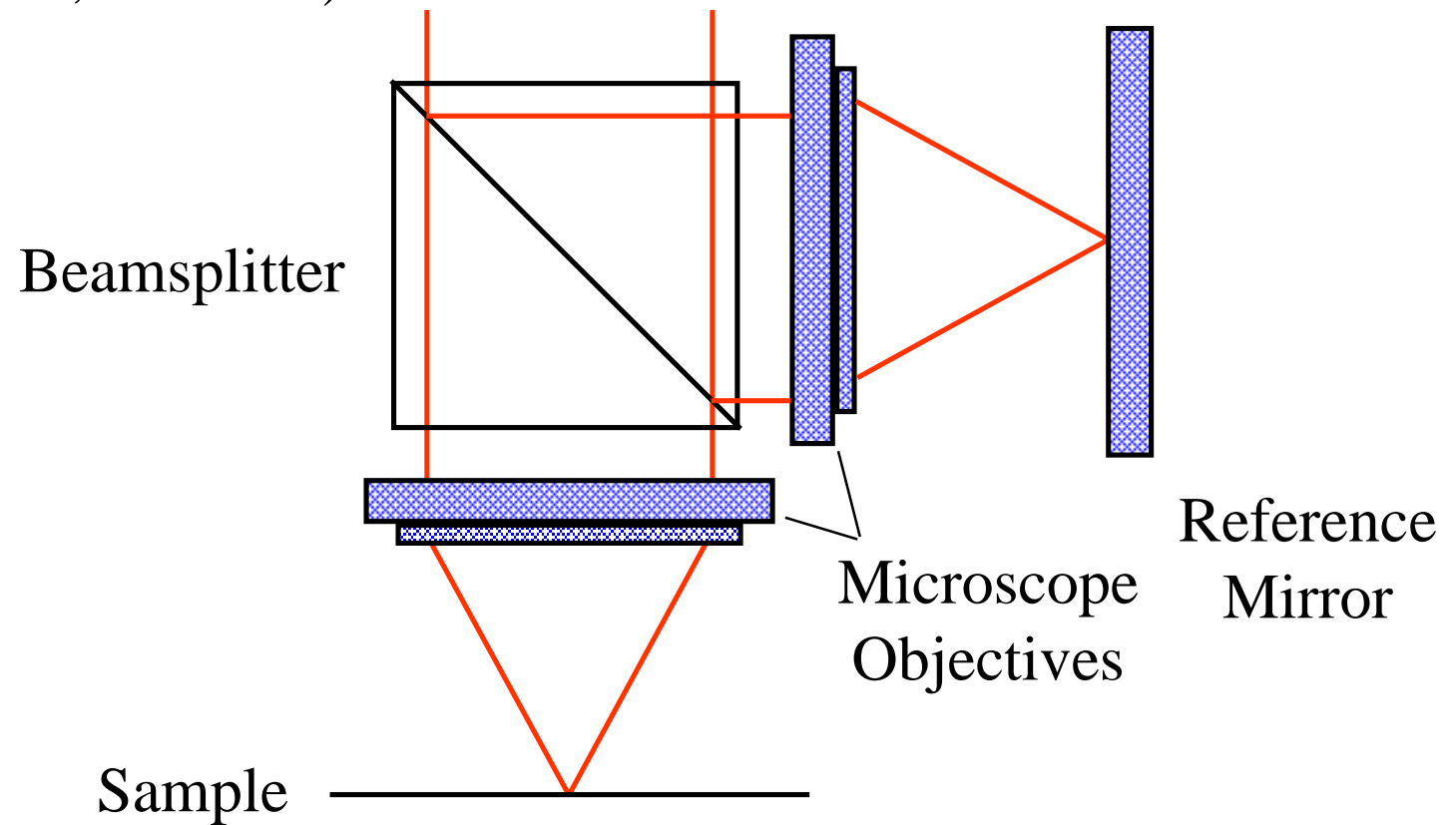
Michelson Interferometer

(1.5X, 2.5X, 5X)



Linnik Interferometer

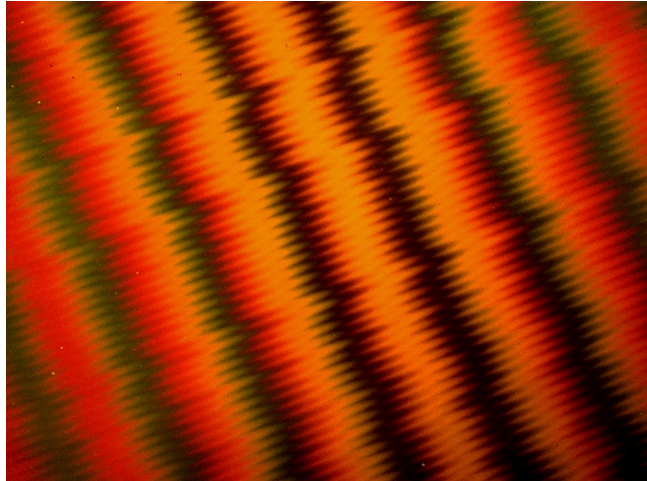
(100 X, NA 0.95)



Interference Objectives

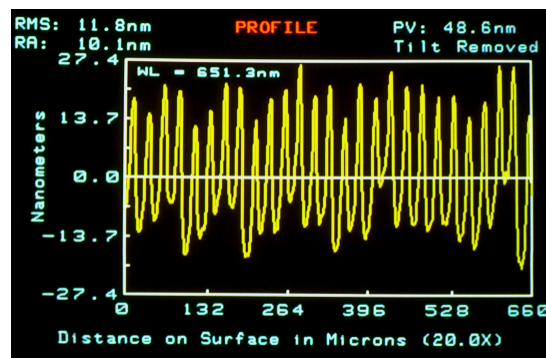
- **Mirau**
 - Medium magnification
 - Central obscuration
 - Limited numerical aperture
- **Michelson**
 - Low magnification, large field-of-view
 - Beamsplitter limits working distance
 - No central obscuration
- **Linnik**
 - Large numerical aperture, large magnification
 - Beamsplitter does not limit working distance
 - Expensive, matched objectives

White Light Interferogram



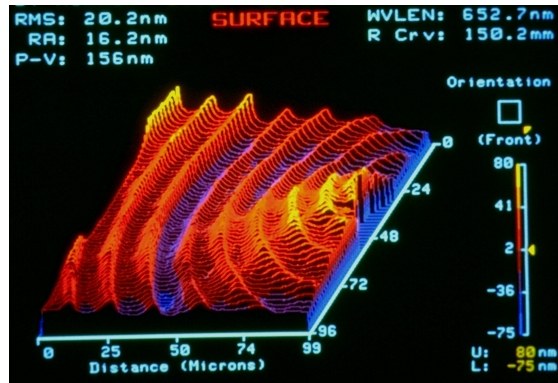
Optics 513 - James C. Wyant

Profile of Diamond Turned Mirror



Optics 513 - James C. Wyant

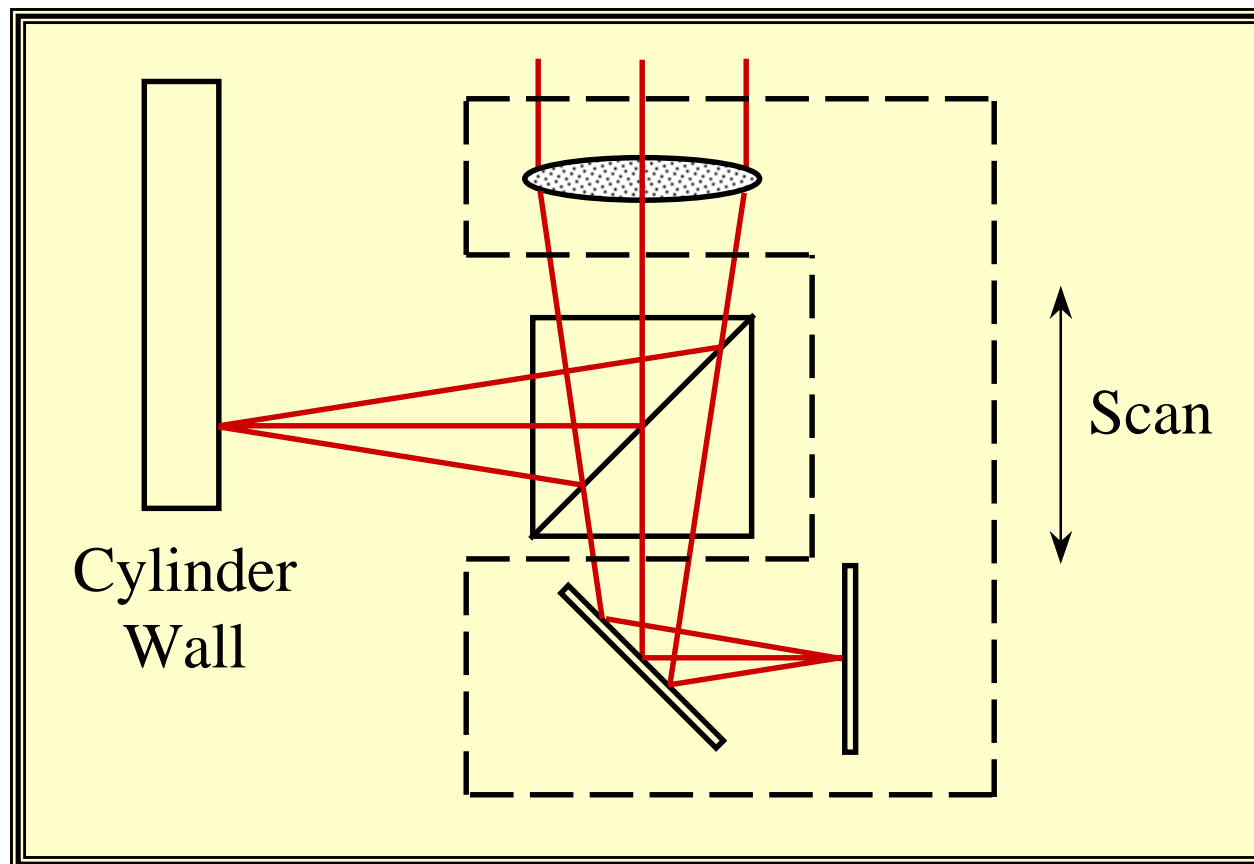
Diamond Turned Mirror



Measurement of Engine Block Cylinder Walls

- Inside of engine block cylinder walls
 - Surface microstructure critical for reduced pollution and increased fuel economy
 - Profile data given by stylus profilometers often not sufficient. Need 3-D information.

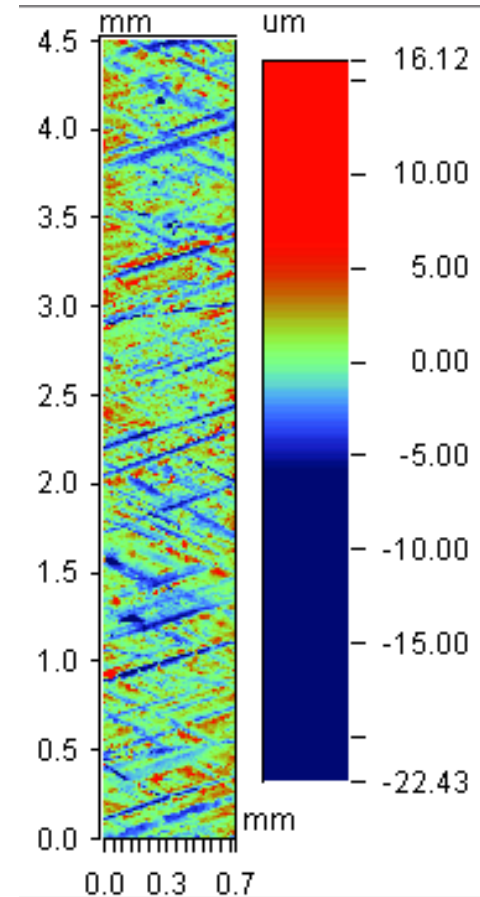
Vertical Scanning



Six Stitched Data Sets of Inside of Engine Bore



Insight 2000 measuring inside of engine bore



$R_a = 1.69 \mu\text{m}$, $R_z = 27.87 \mu\text{m}$,
and $R_t = 38.54 \mu\text{m}$